Article

Not peer-reviewed version

Petrology and Geochemistry of Scandium in Wailukum Ni Laterites, East Halmahera, Indonesia

Abdul Bari * , Mega Fatimah Rosana , Euis Tintin Yuningsih , Ade Kadarusman , Rubima Aisha Yulman , Muhammad Chandra RM , Thaha Rizal Ulhaque

Posted Date: 16 December 2025

doi: 10.20944/preprints202512.1452.v1

Keywords: olivine; pyroxene; scandium; serpentine; ultramafic

 doi:10.20944/preprints202512.1452.v1

Article

Petrology and Geochemistry of Scandium in Wailukum Ni Laterites, East Halmahera, Indonesia

Abdul Bari [1,2,*], Mega Fatimah Rosana [1], Euis Tintin Yuningsih [1], Ade Kadarusman [3], Rubima Aisha Yulman [2], Muhammad Chandra RM [2] and Thaha Riza Ulhaque [2]

[1] Faculty of Geological Engineering, Padjadjaran University, Bandung, Indonesia, 40132

[2] PT. Antam Tbk. Jakarta, Indonesia, 12530

[3] AKA Geosains Consulting, Tangerang, Indonesia, 15311

* Correspondence: abdulbariikawangi@gmail.com

Abstract

The Wailukum area in North Maluku Province, Indonesia, is an ultramafic rock complex with a high degree of serpentinization. The mineral composition of ultramafic and mafic rocks strongly influences scandium (Sc) distribution and enrichment during lateritization. This study aims to analyze the element distribution, mineral composition, and rock identification in three types of geological materials in a lateritic profile which contains Sc, specifically bedrock, saprolite, and limonite. The analytical methods used are petrography, X-ray Diffraction (XRD), X-ray Fluorescence (XRF), Inductively Coupled Plasma (ICP), and Scanning Electron Microscopy – Energy Dispersive Spectroscopy (SEM-EDS). Results show that in the bedrock, Sc is mainly hosted in clinopyroxene minerals such as augite and diopside, with minor amounts in chromite, magnetite, dolomite, and anorthite. In the saprolite, Sc content decreases due to higher mobility but remains partly associated with clinopyroxene and chromite. In the limonite zone, Sc reaches maximum enrichment, primarily hosted in Fe–Mn oxides including goethite, magnetite, and asbolane. Among rock types, gabbro contains the highest absolute Sc concentration (23.25 ppm in bedrock and up to 58.5 ppm in limonite), while wehrlite records the greatest enrichment ratio, with a 9.18-fold increase from bedrock to limonite. In contrast, gabbro shows the lowest enrichment ratio (2.52-fold) despite its high initial Sc content. These patterns indicate that Sc enrichment is controlled by clinopyroxene as the primary host in bedrock, its relative stability during weathering, and the subsequent fixation of Sc in Fe, Cr, and Mn oxides within the lateritization profile.

Keywords: olivine; pyroxene; scandium; serpentine; ultramafic

1. Introduction

Scandium (Sc) is the 21st element in the periodic table, a transition metal and classified as a rare earth element [1]. First identified by Lars Fredrik Nilson in 1879, scandium has a relatively low abundance in the Earth's crust (±22 ppm), but is widely distributed in various rocks, particularly ultramafic rocks [2]. Its content is generally <0.2% in heavy lanthanide ores, tin, uranium, and tungsten, and it has significant economic value through its use in aluminium alloys for the aerospace industry, light vehicles, lighting technology, fuel cells, and sports equipment [3].

Ultramafic rocks consistently contain scandium at an average level of 15.7 ppm, with the highest concentrations found in rocks with high pyroxene content [4]. Several studies [4–8] confirm the close association between scandium and ultramafic rocks, particularly pyroxene and amphibole minerals, through isomorphic substitution of Al or Mg in the crystal lattice.

Previous research by [4] emphasized that during weathering, scandium is mobilized and concentrated in lateritic limonite horizons through residual enrichment and an affinity for iron oxides, particularly goethite. Its concentration can increase significantly from approximately 15 ppm

 doi:10.20944/preprints202512.1452.v1

in basement rocks to approximately 81 ppm in limonite. The primary controlling factors for scandium accumulation are the type of basement rock and its host minerals. In fresh peridotite rocks, enstatite is the dominant host, while in mafic-ultrabasic intrusions, hornblende plays the primary role. In laterite profiles, goethite plays a crucial role in the formation of scandium-rich zones.

Studies from [4,7] also show that the distribution of scandium in pyroxene is influenced by temperature, magma composition, and crystallization sequence. These studies further seek to identify which specific types of pyroxene host higher concentrations of scandium, with the results indicating that clinopyroxene is the primary host.

Present day Halmahera is interpreted as the result of double subduction system between Maluku Sea with Sangihe Arc in the west and Halmahera Arc in the east, this phenomenon subducted almost the entirety of the Maluku Sea and resulted in the emergence of the obducted ophiolite complex in the east of Halmahera Island [9] (Figure 1A). The Wailukum area is located in the East Halmahera geological province, which is characterized by an ophiolite complex and Mesozoic deep-sea sediments, imbricated with Paleogene sediments, and overlain by marine clastic sediments and Neogene carbonates (Figure 1B). The northeast arm of Halmahera island where Wailukum area belongs, consists of dismembered ultramafic-mafic rocks complex with variable low-grade metamorphic overprint and intercalated with Mesozoic and Eocene sediments [10].

Based on local geological mapping by [11], the lithology types in the Wailukum area consists of mixed (melange) rocks, peridotite, serpentinized peridotite, and serpentinite lithological units (Figure 1C). The peridotite unit occupies >60% of the study area, stretching from the north to the south. Some of the peridotite has undergone quite strong serpentinization, and serpentinized peridotite extends to the southeastern part of the study area. In the northeastern part, a melange lithology extends northwest-southeast, directly adjacent to the peridotite. This unit is mixed within the shear zone and is exposed on the Wailukum ridge. Serpentinite is found in the central part of the study area and occupies approximately 10% of the study area. This unit is equated with the Cretaceous ultramafic rock unit [12]. From this results, the ultramafic complex in Wailukum, North Maluku, is estimated to contain significant amounts of scandium. This study aims to analyze the relationship between ultramafic rock type and scandium content through mineralogical studies of three geological horizons: bedrock, saprolite, and limonite.

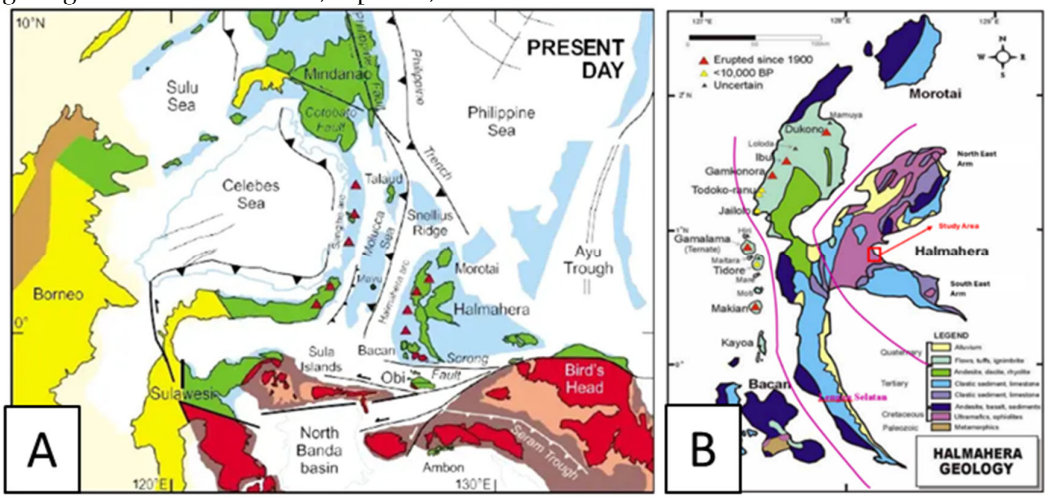

 doi:10.20944/preprints202512.1452.v1

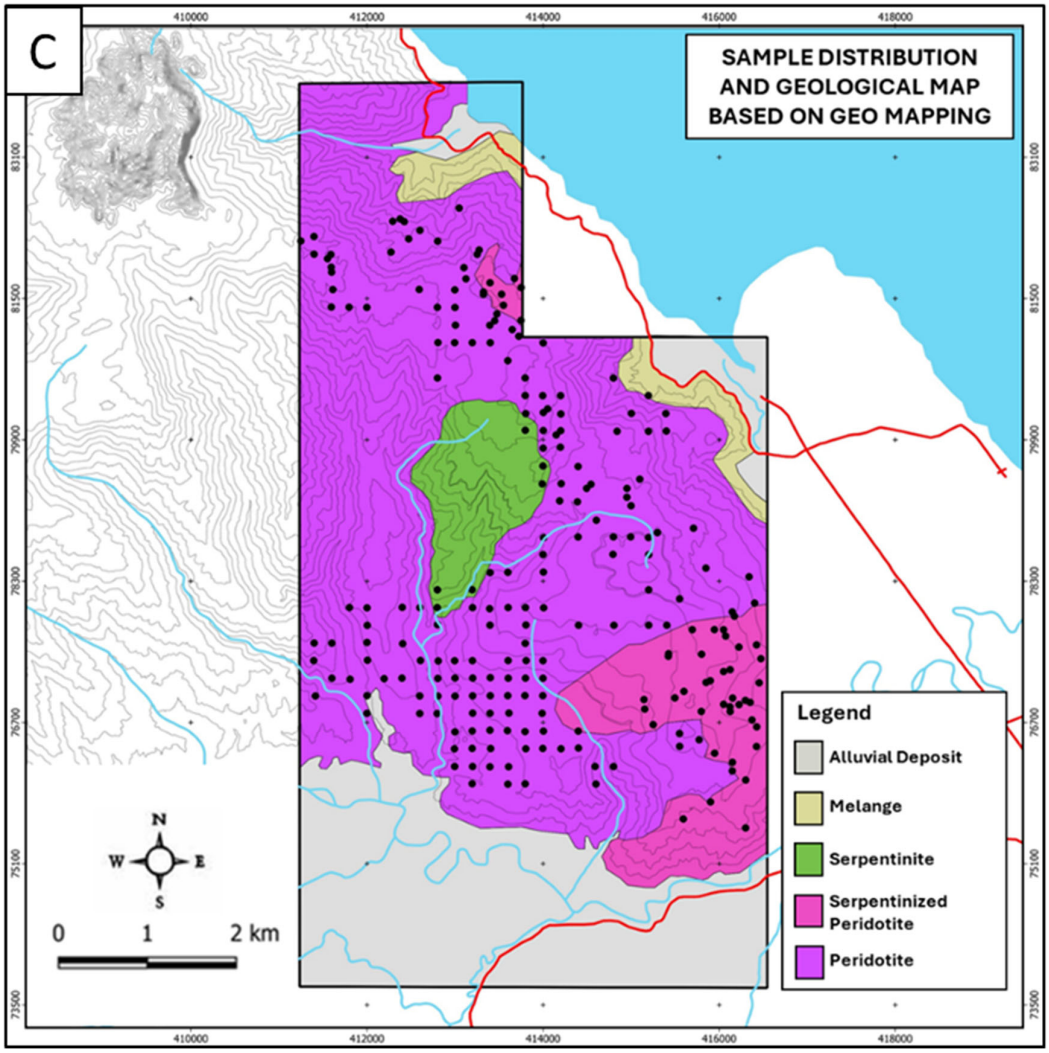

Figure 1. A. Regional tectonic setting of Halmahera and surrounding region (Hall, 2000); B. Geological map and distribution of ultramafic rocks in East Halmahera Regency, North Maluku (Turdjaja et al., 2011); C. Local geological map of the Wailukum research area and location of sampling points from drill data (modified from Antam, unpublished report).

2. Materials and Methods

This research was conducted through direct field data collection by conducting geological mapping and drilling across the research area (Figure 1C). This study collected 712 samples from 270 drill holes in the Wailukum area, North Maluku, Indonesia. There are 231 bedrock samples from 270 drill points that are grouped and then further studied as a basis for naming and distributing rocks in the study area. Core sampling was conducted using the single-tube drilling method, with whole core sampling taken at 1 meter intervals. Core samples were NQ in size with a diameter of approximately 6 cm. Each drill data set was sampled at intervals representing each zone. These zones are distinguished by the degree of rock weathering, namely limonite, saprolite, and bedrock zones.

A total of 712 samples from 270 drill holes were prepared through preparation process using jaw crusher and pulverizer to obtain a representative #200 mesh pulp sample. Laboratory analysis was conducted at PT Aneka Tambang Tbk.'s internal laboratory and the Intertek Laboratory using X-Ray Fluorescence (XRF), Inductively Coupled Plasma – Optical Emission Spectroscopy (ICP-OES), and X-Ray Diffraction (XRD) methods, as well as at the Geoservices Laboratory using Scanning Electron Microscope – Energy Dispersive Spectroscopy (SEM-EDS).

 doi:10.20944/preprints202512.1452.v1

The method used for petrographic analysis begins with preparing a thin section by cutting a rock slab (3 × 3 cm), grinding it to about 30 μm thickness so silicate minerals show their optical properties, and mounting it on a glass slide with adhesive and a coverslip. The thin section is then examined under a polarized light microscope Olympus BX51 and Nikon Eclipse LV100 Pol. This method allows identification of mineral types, estimation of their relative abundances, and observation of textural relationships such as grain size, shape, and arrangement.

The XRF method using the Panalitycal Axios Fast Wavelength Dispersive X-Ray Fluorescence (WDXRF) instrument produced quantitative data on major elements in oxide form, such as Fe_2O_3, SiO_2, MgO, CaO, MnO, Cr_2O_3, Al_2O_3, P_2O_5, SO_3, also in base metal form, such as Ni and Co.

The ICP-OES method, a plasma-based analytical technique for detecting metallic elements in ppm units, was used to analyze minor elements, including the presence of scandium.

XRD analysis using a Bruker D8 Advance instrument identified mineral composition based on X-ray diffraction patterns. The diffraction data were analyzed against the International Centre for Diffraction Data (ICDD) 2022 database using diffract. EVA v6.1 and Topaz v6.1 software. The results were calculated using the Rietveld refinement approach to quantify mineral phases, particularly in laterite samples that had undergone advanced weathering.

SEM-EDS analysis combines electron imaging with X-ray mapping to identify scandium-bearing minerals. This technique allows detailed observation of element and mineral associations through mapping and spot analysis.

3. Results

3.1. Mineralogy Observations

3.1.1. Petrographic Analysis

Petrographic analysis on several samples shows at least three lithologies were identified on the research area, they are dunite, serpentinite, and harzburgite.

Dunite is a type of ultramafic igneous rock consisting of olivine as the main mineral in rock formation, the presence of this mineral can reach 90% of the total minerals present in the rock. In the research area, the condition of this rock is generally dark gray-brownish (Figure 2A-B), there are many fractures or cracks, the dominant composition is olivine with medium to coarse mineral size, granular, has a low magnetic response, some of these fractures are filled by serpentine and form a mesh texture. The results of microscopic observation on this dunite rock show the presence of serpentinization from moderate to high, phaneric with medium to coarse mineral sizes (0.2 – 2 mm), holocrystalline, subhedral to euhedral, with the main mineral composition of olivine, with orthopyroxene mineral accessories, and a high degree of fracture, showing a mesh texture together with serpentine (Figure 2C-D).

 doi:10.20944/preprints202512.1452.v1

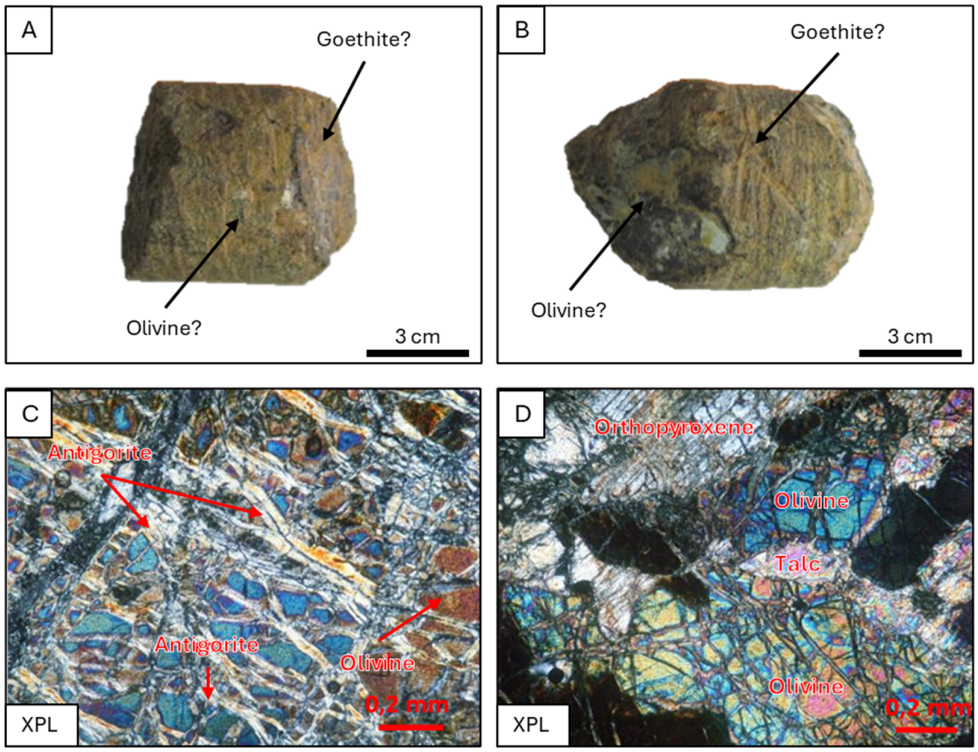

Figure 2. A-B. Handspecimen photo of dunite; C-D. photomicrocraph of coarse-grained olivine and accessory orthopiroxene. Olivine exhibits numerous fractures that have been transformed into antigorite (serpentinite).

In the southeastern part of the observation area, bordering the hazburgite rock area, a group of serpentinite rocks was observed. This rock is light green to dark green, which appears to have whitish fractures (Figure 3A). Serpentinite, a holocrystalline, equigranular, fine-grained, fibrous mineral, consists of serpentine that alters the entire sample, and this mineral is also present as filler in the vein zones that cut through this rock. Between these serpentine veins are fine-grained chlorite veins that follow the serpentine vein path (Figure 3B). The presence of serpentine minerals in each rock group is quite high, but in serpentinite-type rocks, they are grouped based on the presence of serpentine and kaolinite-serpentine mineral groups such as talc with a total presence of more than >90% of the total rock minerals.

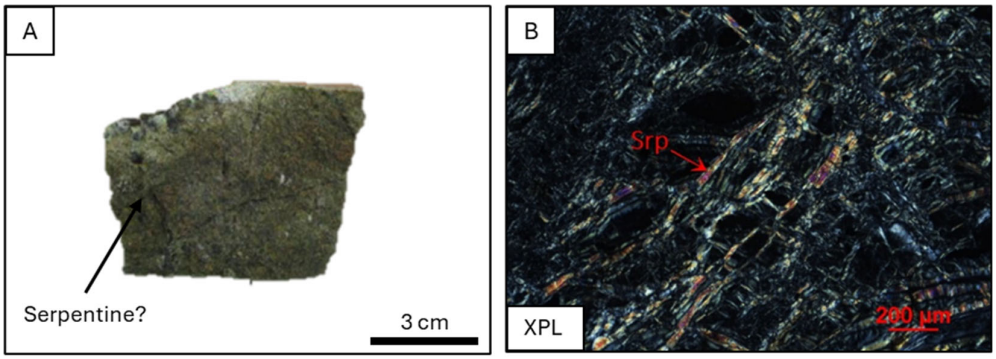

Figure 3. A. Handspecimen photo of serpertine; B. Photomicrograph of fibrous serpentine.

Harzburgite specimen found in the research area appear dark green to brownish gray, composed predominantly of olivine, pyroxene, and in many cases, partially altered to serpentine. It has a medium to coarse granular texture with abundant fractures, medium to coarse granular texture, and relatively low magnetic response. The serpentine mineral filled the fractures, producing a mesh texture typical of altered peridotites (Figure 4A-B).

 doi:10.20944/preprints202512.1452.v1

Under microscope, most of the mineral observed are olivine and orthopyroxene, with a relatively high presence of serpentine, reaching 70% of the total mineral content. Microscopic observations (Figure 4C-F) show the presence of highly fractured olivine and orthopyroxene, with the presence of serpentine altering olivine and serpentine in the weak planes of these two primary minerals. Weathering is quite low with the presence of iddingsite minerals at several points that change olivine minerals, also observed in polished sections the presence of opaque chromite minerals with low intensity.

Olivine is present colorless, with thick relief, and double refraction of 2nd -3rd order, many fractures are visible between olivine, while orthopyroxene is present with a slightly greenish color, or reddish-colorless pleochroic, with visible cleavage in one direction. In the weak plane of these two minerals, alteration of serpentine minerals is seen forming a mesh structure. Fibrous serpentine is present filling between the weak planes of olivine, the presence of brownish oxide minerals in the form of iddingsite (minor) is seen. The mesh structure or what is also commonly termed as sea and island is very clearly visible in sample PET004. The presence of talc as an alteration mineral in addition to the presence of serpentine minerals. Talc, colorless, low relief, very high double refraction, very fine in size. Chromite appears to be distributed spotted among the other rock constituent minerals, with very low intensity (<1%) (Figure 4C-F).

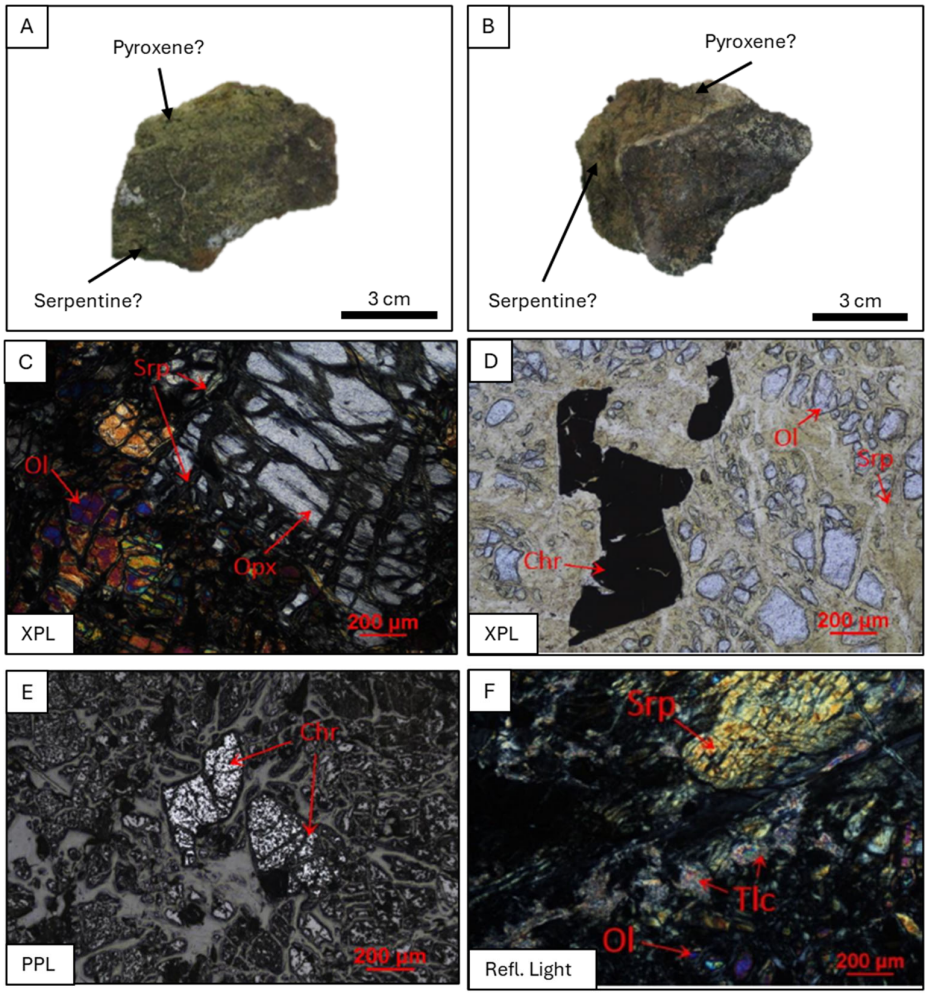

Figure 4. A-B. Hand specimen photo of harzburgite; C-F. Photomicrograph of harzburgite rocks in the basement zone.

 doi:10.20944/preprints202512.1452.v1

3.1.2. XRD Analysis

On the basis of XRD analysis, there are at least 6 identified patterns based on the consistent variations of mineral spectrum (Figure 5). Type 1 spectrum is characterized by the occurrence of talc, forsterite, fayalite, diopside, enstatite, kaolinite, lizardite, and chlorite (Figure 5A). The X-ray diffraction pattern for sample BL31701 (Type 1) displays a complex assemblage of crystalline phases, as indicated by a series of well-defined peaks distributed between 5° and 60° 2θ. The diffraction profile is characterized by several high-intensity reflections, most notably the dominant peak near 11–12° 2θ and additional strong spectrum at approximately 25°, 36°, and 38° 2θ. These primary peaks suggest the presence of a mixed silicate mineralogy typical of serpentinized ultramafic lithologies. Overlaying the measured pattern are reference peak positions for eight candidate minerals: forsterite, fayalite, diopside, enstatite, kaolinite, lizardite, talc, and chlorite. Peak correspondence indicates that multiple phases contribute to the overall diffraction signal. The forsterite–fayalite series is represented by peaks in the 10–12° and 35–37° regions, consistent with Mg-Fe olivine components. Pyroxenes (diopside and enstatite) exhibit diagnostic reflections clustered between 28–32° and 36–40° 2θ, aligning closely with several medium-intensity peaks in the measured spectrum. Low-temperature alteration minerals—including lizardite, talc, and chlorite—are identified by characteristic peaks between ~7–10°, 18–20°, and 24–26° 2θ, corresponding with observed broad and moderate-intensity features. The presence of kaolinite is suggested by minor reflections near 12° and 24°. The combined pattern reflects partial serpentinization and hydrothermal alteration of a primary ultramafic protolith, producing an assemblage of olivine-pyroxene relicts overprinted by sheet silicates and hydrous Mg-phases.

Type 2 spectrum is characterized by the occurrence of talc, forsterite, fayalite, augite, diopside, enstatite, kaolinite, lizardite, talc, and tremolite (Figure 5B). The X-ray diffraction (XRD) pattern of sample BL85447-O (Type 2) illustrates the strongest reflections occur between ~28° and 38° 2θ, where overlapping peaks from orthopyroxene- and clinopyroxene-group minerals (augite, diopside, enstatite) coincide with olivine-group phases (forsterite, fayalite). Additional peaks at lower angles (~8°–15° 2θ) correspond to phyllosilicate minerals (kaolinite, lizardite, talc), indicating the presence of alteration products.

Type 3 spectrum is characterized by the occurrence of forsterite, fayalite, diopside, enstatite, kaolinite, lizardite, talc, and chlorite (Figure 5C). the X-ray diffraction (XRD) pattern of sample BL86369-Q (Type 3) shows the distribution of diffraction peaks associated with major silicate and phyllosilicate mineral phases. Prominent peaks occur at approximately 10°–12° 2θ and 25°–35° 2θ, where phyllosilicate minerals such as chlorite and serpentine-group phases produce their characteristic and high-angle reflections. Additional sharp peaks between ~30° and 40° 2θ are consistent with pyroxene minerals (augite, diopside, enstatite), suggesting the presence of relatively unaltered mafic silicate components.

Type 4 spectrum is characterized by the occurrence of forsterite, fayalite, kaolinite, lizardite, talc, and chlorite (Figure 5D). the X-ray diffraction (XRD) pattern of sample BL86466-O (Type 4) reveals strong reflections occur in the 28°–36° 2θ range, where the overlap of pyroxene-group minerals (augite, diopside, enstatite) contributes to multiple coincident peaks. Additional peaks at ~10°–12° 2θ correspond to basal spacings of chlorite and serpentine minerals, indicating the presence of alteration phases. Higher-angle reflections extending beyond 40° 2θ further support a heterogeneous composition containing both Mg-Fe silicates and phyllosilicates.

There are 4 (four) bedrock samples containing high plagioclase presence. In the XRD analysis results it is seen that the presence of feldspar (anorthite), pyroxene (aegirine, diopside, augite), serpentinite (lizardtite), and clay minerals such as kaolinite and chlorite. Most of the spectrum are concentrated around 20° – 35° 2θ. The presence of this mineral assemblage is classified as gabbro.

The last patten of XRD shows the dominance of lizardite with talc mineral and chlorite (Figure 5F). These mineral assemblages indicate that the bedrock is already classified as serpentinite.

From these patterns, we also used the Rietveld refinement (Figure A1) approach to quantify mineral phases which then we plot the data to Streickesen diagram (1972) (Figure 6) [13]. The results

 doi:10.20944/preprints202512.1452.v1

from this analysis are type 1 samples are classified into dunite, type 2 samples are classified into harzburgite, type 3 samples are classified into lhezorlite, and type 4 samples are classified into wehrlite. The data for type 5 and 6 are not plotted into the streickesen diagram since the mineralogical characteristics already distinguished as gabbro, for type 5 samples, and as serpentinite, for type 6 samples.

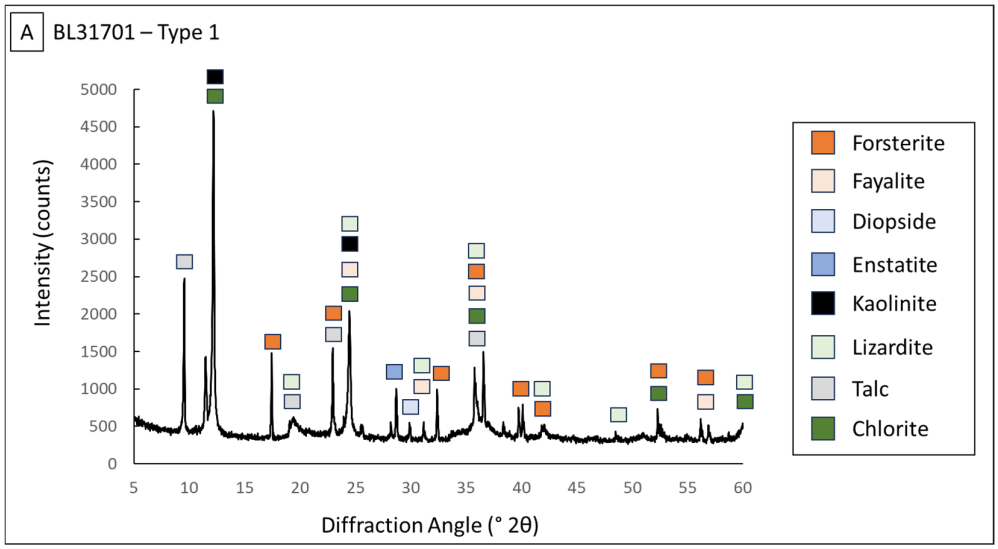

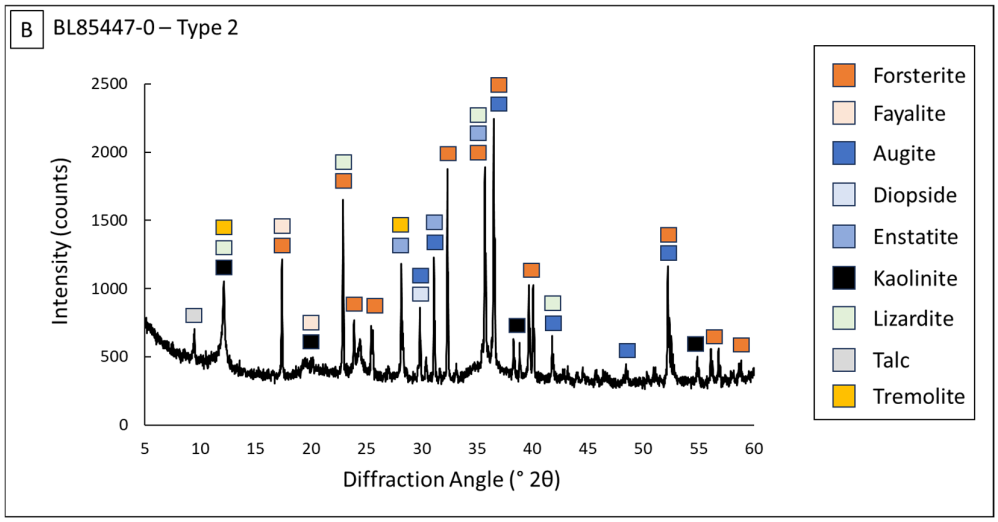

 doi:10.20944/preprints202512.1452.v1

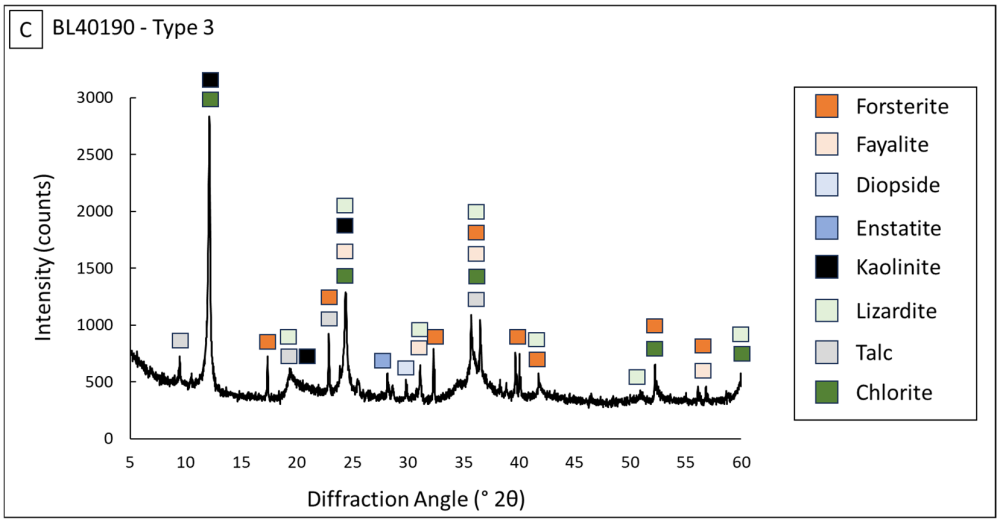

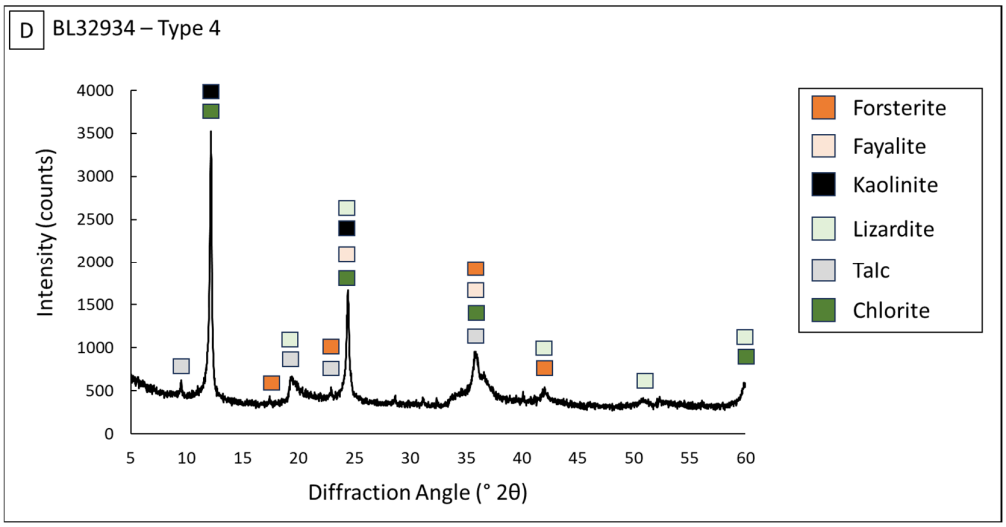

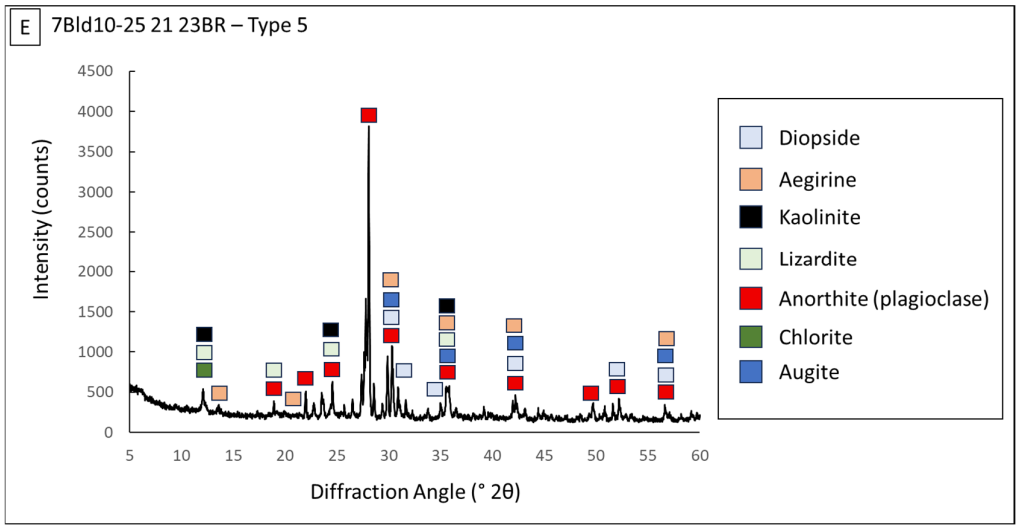

 doi:10.20944/preprints202512.1452.v1

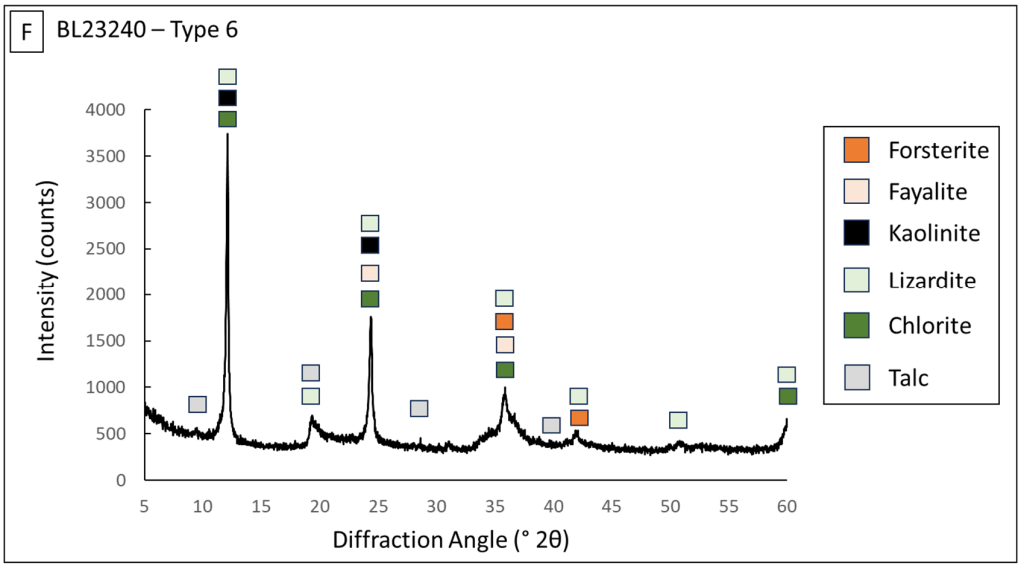

Figure 5. A-C. Representative of different types of XRD pattern in Wailukum research area. D-F. Representative of different types of XRD pattern in Wailukum research area.

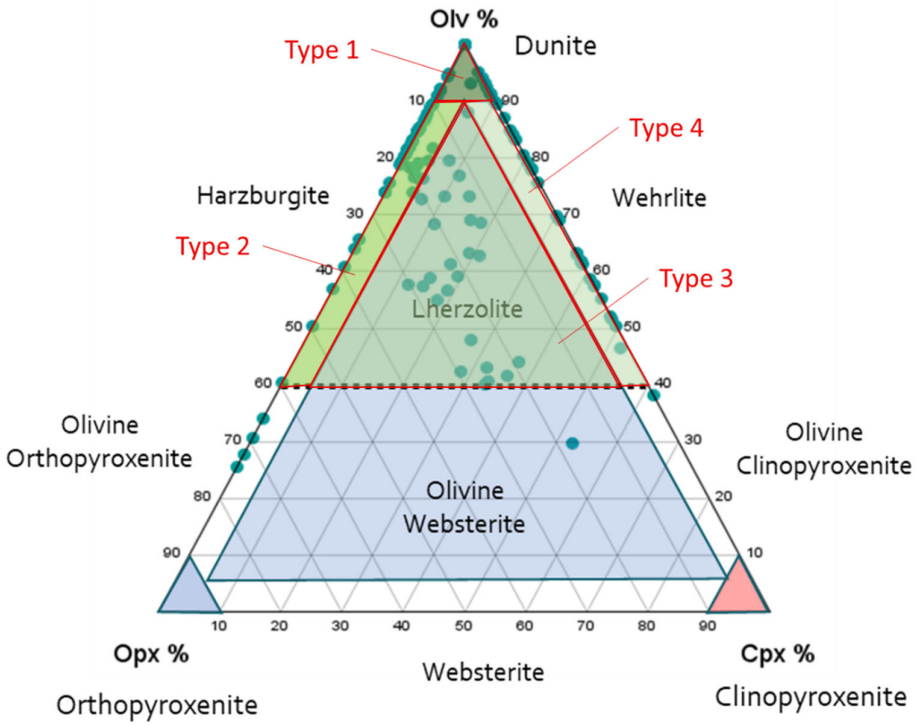

Figure 6. Distribution of bedrock types in the Wailukum area based on XRD analysis of bedrock, using Rietveld refinement method (modified from Streickesen,1975).

3.1.3. SEM-EDS Analysis

On the basis of Scanning Electron Microscopy - Energy Dispersive X-Ray Spectroscopy (SEM-EDS) analysis combined with elemental mapping, the scandium occurs in as isomorphic substitution sites within the crystal structures of clinopyroxenes, namely diopside and augite.

Elemental mapping using Energy-Dispersive Spectroscopy (EDS) for Sc (Figure 7A-B) shows enhanced Sc signals within this mineral, suggesting possible incorporation of scandium; however, the concentrations remain below the detection limit of the instrument, preventing precise

 doi:10.20944/preprints202512.1452.v1

quantification. A similar feature was observed in the wehrlite bedrock, where grains identified as augite altered into serpentine. In the preserved remnants of primary augite, the presence of scandium was still detected, indicated by increasingly intense green coloration in the mapped area (Figure 7C-D).

In the saprolite zone, several SEM observations revealed that scandium remains locally bound within primary minerals such as clinopyroxene (diopside). However, in most cases, this element appears to have been leached and subsequently enriched within chromite. In SEM analysis of lherzolite from the saprolite horizon, BSE imaging displayed bright white areas of very high contrast (Figure 7E-F), indicating the presence of highly conductive mineral phases. EDS analyses at these points detected high Fe concentrations with minor Cr and Mn, along with localized Sc signals concentrated in these regions. This association is interpreted as iron-rich mineral phases with Cr-Mn-Sc impurities.

In the limonite zone, scandium occurs in a wider variety of host minerals and is predominantly associated with oxides such as chromite, magnetite, goethite, and asbolane (Figures 7G-H). In addition to these oxides, scandium is also observed to remain bound within residual primary minerals, including diopside in dunite and augite in gabbro. Beyond the remnants of these primary phases, scandium is further incorporated into secondary minerals formed through lateritization, such as chromite, goethite, native iron, and notably asbolane (Mn(O,OH)2(Ni,Co)X(O,OH)2 .nH20).

Gabbro rock group however, has a very small distribution in the sample, as seen in Table 1, the presence of Gabbro was only identified in 4 samples out of a total of 231 samples that were subjected to mineralogical observations, and is the sample with the highest Scandium content with a presence of 30 ppm in the bedrock, and increasing to 70 ppm in the limonite zone. Meanwhile, in the other five rock groups, the average presence of Scandium does not show much difference, in the bedrock zone.

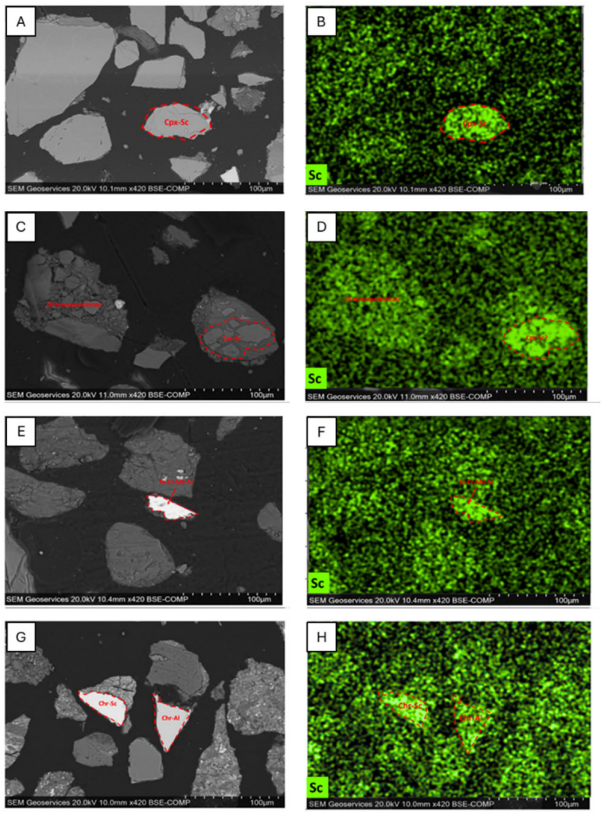

 doi:10.20944/preprints202512.1452.v1

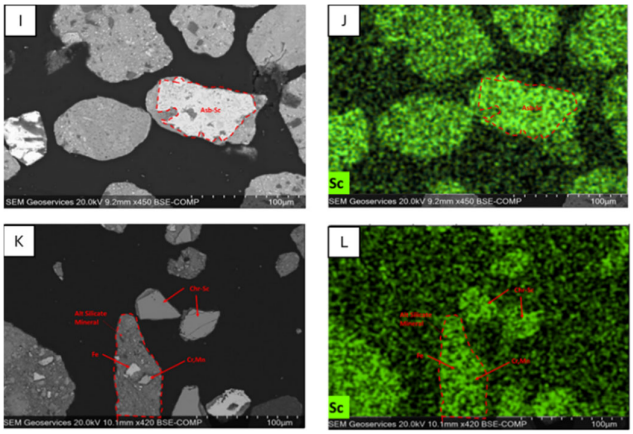

Figure 7. Image of backscattered electron (BSE) and the elemental mapping of scandium (Sc) (caption continues to the next page). (A-B) harzburgite bedrock, the observed distribution of Sc elements is present in the minor mineral diopside; (C-D) wehrlite bedrock, the observed distribution of Sc is present in Augite which has begun to weather into serpentinite?; (E-F) lhezorlite saprolite zone, the observed concentration of Sc is present in iron minerals; (G-H) wehrlite saprolite zone, the presence of a chromite that binds scandium and a chromite that does not bind scandium is visible; (I-J) wherlite limonite zone, the presence of scandium minerals is seen in the asbolane minerals; (K-L) lhezorlite limonite zone, the presence of scandium minerals is seen in chromite minerals.

Table 1. The presence of scandium in each type of rock based on SEM-EDS observation results.

Rock Type	Laterite Zone	Diopside	Augite	Chromite	Magnetite	Iron	Goethite	Asbolane
Dunite	Limonite	+				+		
Dunite	Saprolite	+		+				
Dunite	Bedrock	+	+					
Harzburgite	Limonite			+				
Harzburgite	Saprolite	+						
Harzburgite	Bedrock	+	+					
Wehrlite	Limonite			+		+		+
Wehrlite	Saprolite			+				
Wehrlite	Bedrock		+	+				
Lherzolite	Limonite			+			+	+
Lherzolite	Saprolite					+		
Lherzolite	Bedrock			+				
Serpentinite	Limonite			+			+	+
Serpentinite	Saprolite			+				
Serpentinite	Bedrock	+						
Gabbro	Limonite		+	+	+			
Gabbro	Saprolite		+					
Gabbro	Bedrock		+					

3.2. Bulk Geochemistry

The results for bulk geochemical analysis using X-ray Fluorescence (XRF), which measures the overall concentration of major and trace elements in the rock, are summarized in Figure 8 and Table 2. The results indicate that scandium occurs with the highest intensity in gabbro, whereas the lowest degree of enrichment is observed in wehrlite, with an enrichment factor of 9.18 times in the limonite zone compared to the bedrock. Similarly, lherzolite shows an enrichment factor of 8.07 times in the limonite zone relative to the bedrock.

 doi:10.20944/preprints202512.1452.v1

The geochemical composition of the ultramafic rock groups (dunite, harzburgite, lherzolite, serpentinite, and wehrlite) shows consistently low scandium concentrations (5.26–7.03 ppm) with broadly similar levels of Fe_2O_3 (7.70–8.42%), SiO_2 (38.66–43.50%), and MgO (38.69–40.03%). Among them, harzburgite contains the highest scandium content (7.03 ppm), whereas wehrlite has the lowest (5.26 ppm). dunite is distinguished by its high MgO (40.03%), consistent with its olivine rich mineralogy, while lherzolite and wehrlite record slightly higher CaO values (0.22–0.24%), reflecting greater pyroxene proportions.

In contrast, gabbro exhibits a markedly different geochemical signature, with scandium enrichment averaging 23.25 ppm, substantially higher than in the ultramafic groups. This enrichment is coupled with elevated CaO (11.16%) and reduced MgO (16.01%), consistent with its clinopyroxene and plagioclase rich mineralogy. The low Ni content in Gabbro (0.11%) relative to the ultramafic rocks (0.27–0.34%).

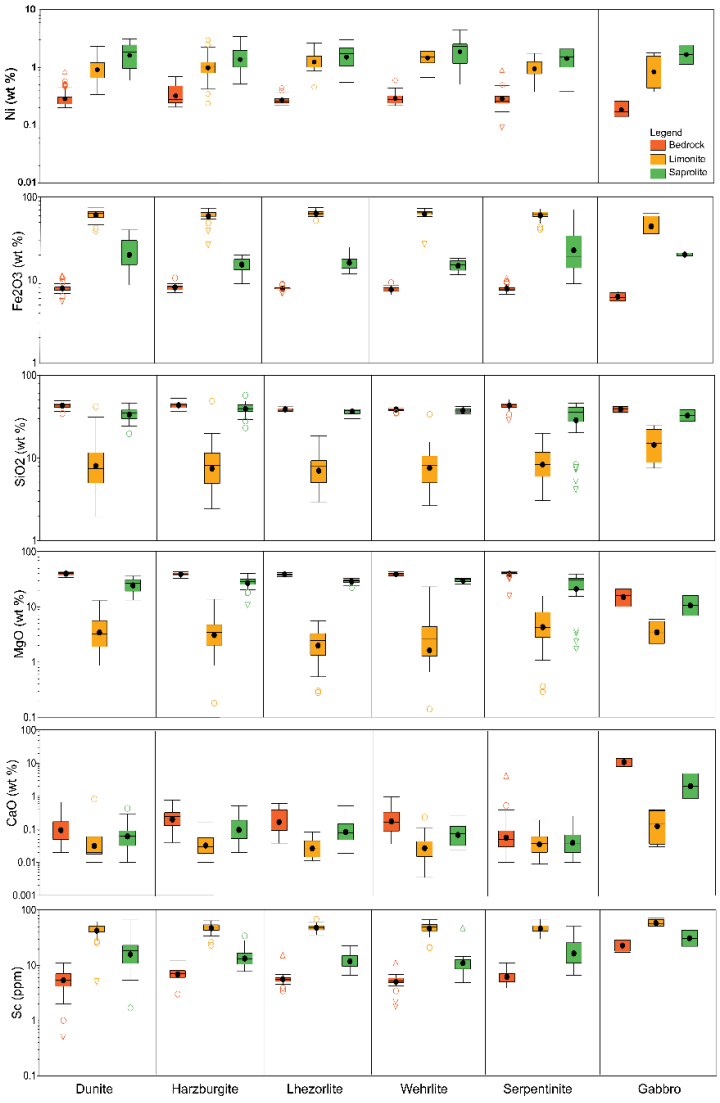

Figure 8. Representative XRF data of each horizon in Wailukum area.

 doi:10.20944/preprints202512.1452.v1

Table 2. The composition of major elements in the rock groups in the Wailukum area and their comparison with the Scandium and Nickel levels in the bedrock zone.

Rock Groups	Laterite Zone	Sampel Quantity	Average Composition					
			Scandium (ppm)	Ni (%)	Fe2O3 (%)	SiO2 (%)	MgO (%)	CaO (%)
Dunite	Limonite	42	44.55	0.98	49.14	9.60	4.66	0.06
	Saprolite	34	18.95	1.77	18.13	33.13	24.86	0.08
	Bedrock	68	5.83	0.30	6.55	43.25	40.08	0.12
Harzburgite	Limonite	38	47.86	1.11	36.75	9.25	4.00	0.04
	Saprolite	28	14.29	1.55	9.51	39.67	26.97	0.14
	Bedrock	45	7.03	0.34	4.96	43.45	39.18	0.24
Lherzolite	Limonite	25	48.28	1.31	63.98	7.75	2.53	0.03
	Saprolite	25	12.09	1.69	16.48	36.51	28.92	0.11
	Bedrock	25	5.26	0.28	7.89	38.72	38.69	0.23
Wehrlite	Limonite	29	46.89	1.51	63.48	8.97	3.21	0.04
	Saprolite	26	12.27	2.08	15.20	37.35	29.82	0.08
	Bedrock	26	5.81	0.30	7.74	38.64	38.97	0.25
Serpentinite	Limonite	40	48.05	0.99	41.41	9.33	5.76	0.06
	Saprolite	33	19.28	1.55	22.62	31.27	24.92	0.05
	Bedrock	61	6.33	0.32	5.56	42.12	38.96	0.17
Gabbro	Limonite	2	58.50	0.57	45.67	15.65	3.76	0.20
	Saprolite	4	32.50	1.04	20.32	33.02	11.53	2.86
	Bedrock	4	23.25	0.11	6.30	38.93	16.01	11.16

4. Discussion

4.1. XRD Data Application in Laterite Geological Mapping

The initial geological maps, which were constructed through macroscopic observations and field surveys (Figure 1C) were substantially refined by integrating data from XRD and petrography analyses. As demonstrated in Figure 9, the updated maps delineate more detail lithological. The combined XRD and petrographic results reveal the presence of specific mineral subgroups, such as fayalite and forsterite within the olivine group, and clinopyroxene and orthopyroxene within the pyroxene group, that are not easily identified during the field or macroscopic observations.

These mineralogical distinctions indicate that area previously classified as “ultramafic rocks” or “peridotites” can be further classified bas on its specific mineralogical variations [13,14]. These compositional variations highlight the interplay between primary igneous processes and subsequent weathering alteration, which are crucial for laterite deposits [15]. The integration between Rietveld-refined XRD data with petrographic observations provides a better exploration to narrow the potential for the occurrence of laterite deposit such as nickel and scandium, as previously mentioned by [16]. Since most of the samples in the Wailukum laterite are heavily weathered and thin section samples are hard to produce, this kind of approach is helpful and give more reliable results compare with the previous results from field observation.

 doi:10.20944/preprints202512.1452.v1

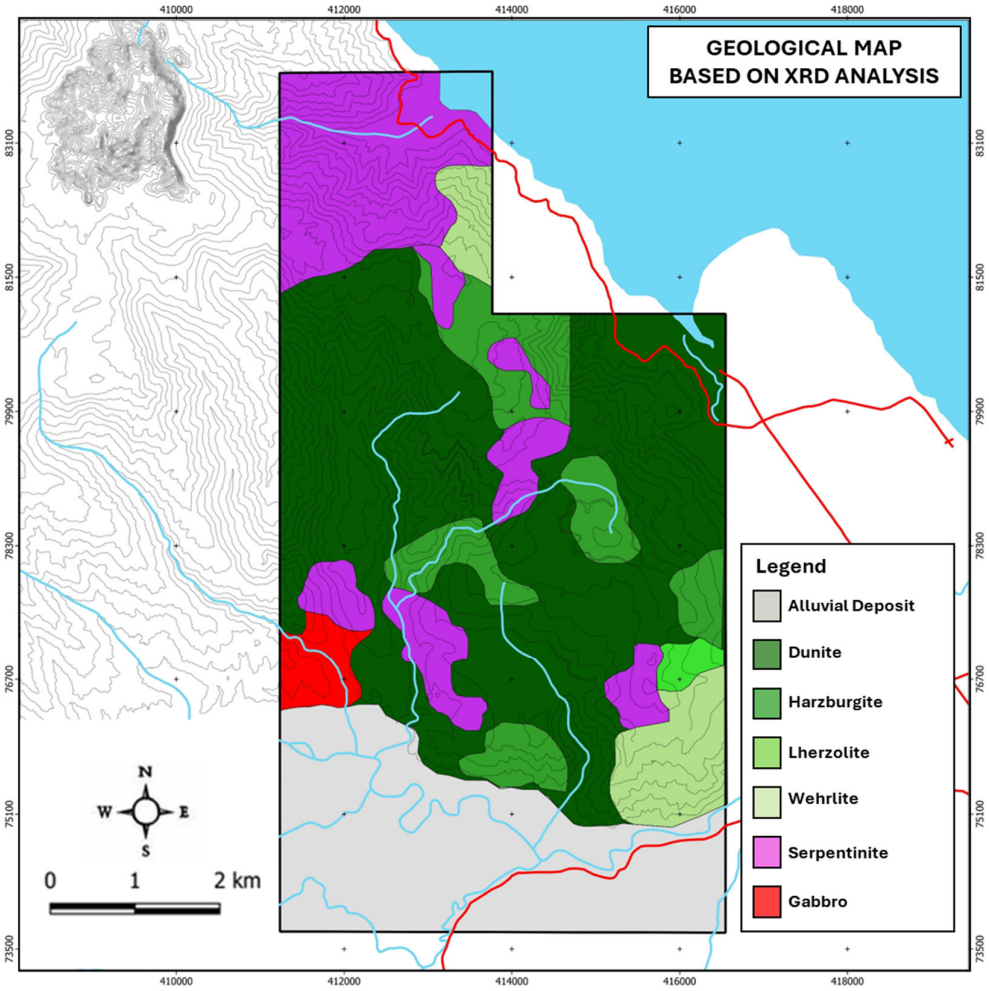

Figure 9. Geological map of the research area based on the results of XRD analysis.

4.2. The Importance of Protolith for Scandium Concentration

In the study area, an ultramafic igneous complex, scandium occurs in association with Fe-bearing minerals such as magnetite and clinopyroxene through the ionic substitution of Fe^{3+} by Sc^{3+}, facilitated by their comparable ionic radii (Sc^{3+} = 0.745 Å; Fe^{3+} = 0.645 Å) [16]. During the crystallization of mafic to ultramafic magmas, scandium tends to concentrate in iron–titanium oxide minerals, particularly magnetite and ilmenite, during the late stages of magmatic differentiation [17].

Mineralogical analyses indicate the presence of anorthite, dolomite, and magnetite within ultramafic and gabbroic lithologies, where scandium incorporation is primarily controlled by magmatic crystallization processes, hydrothermal alteration, and the physicochemical conditions of the formation environment [17].

In primary ultramafic basement rocks such as dunite, harzburgite, wehrlite, lherzolite, and serpentinite—characterized by low clinopyroxene abundance—the scandium content is typically 5–8 ppm, increasing to as much as 23 ppm in gabbroic rocks. This enrichment reflects the critical role of clinopyroxene in hosting scandium during magmatic solidification [17]. In Wailukum area, the order of Sc concentation in bedrock from the lowest to the highest are lhezorlite < wherlite < dunite < serpentinite < harzburgite < gabbro. The pattern shows different order with ultramafic complex in the eastern Australia where the order is dunite < peridotite < gabbro/basalt < amphibolite/pyroxenite [18].

In Wailukum area, lithologies such as lherzolite and wehrlite contain higher proportions of olivine and lower amounts of aluminous phases, resulting in limited Sc incorporation during magmatic crystallization. Their higher susceptibility to weathering promotes earlier release of scandium from silicate lattices, followed by its redistribution into secondary Fe oxyhydroxides in the

 doi:10.20944/preprints202512.1452.v1

saprolite and limonite zones [19]. This process decreases the residual Sc concentration in the primary bedrock but enhances enrichment in the weathering products.

In contrast, ultramafic complexes in eastern Australia display a different Sc trend due to variations in parent magma chemistry and metamorphic overprinting [18]. There, scandium enrichment is commonly associated with Fe–Ti oxide minerals in more evolved basaltic and amphibolitic lithologies rather than in peridotitic units. The divergence in the Wailukum sequence therefore underscores the importance of local magmatic evolution, degree of serpentinization, and intensity of lateritic weathering in governing Sc distribution.

Furthermore, the higher Sc concentration in serpentinite compared to dunite and lherzolite suggests that secondary processes, such as serpentinization and subsequent oxidation, can enhance scandium retention by generating Fe-rich alteration minerals (goethite, magnetite, and asbolane) capable of adsorbing or incorporating Sc^{3+} [20]. The relative stability of these secondary hosts within the weathering profile contributes to the preservation of scandium in serpentinite-derived laterites.

Overall, the observed pattern indicates that scandium distribution in the Wailukum complex is not solely controlled by primary mineralogy but also by the interplay of magmatic differentiation, alteration history, and secondary mineral formation during tropical laterization. This multi-stage control contrasts with the Australian systems, where igneous fractionation and metamorphic re-equilibration dominate scandium partitioning in the bedrock sequence.

4.3. Scandium Enrichment in Laterization Process

In the study area, clinopyroxene and chromite within ultramafic bedrock exhibit greater resistance to lateritization than olivine, allowing scandium to remain bound to these primary minerals within the saprolite zone. In lithologies such as dunite, harzburgite, and serpentinite, olivine which is a highly unstable mineral under tropical weathering conditions will undergoes preferential alteration, releasing Fe, Mg, and other mobile elements, while scandium remains structurally incorporated in the more resistant clinopyroxene and chromite phases [18] and [21,22].

The vertical geochemical profile, encompassing bedrock, saprolite, and limonite zones, reveals that scandium enrichment generally parallels the distribution of Fe and Ni (Figure 8). As weathering progresses, the dissolution of Sc^{3+} from primary silicates facilitates its remobilization in meteoric waters through fractures and pore networks. In saprolitic horizons derived from clinopyroxene-rich wehrlite and lherzolite, scandium persists in association with residual minerals such as clinopyroxene, chromite–spinel, magnetite, and asbolane [20]. The saprolite zone thus represents a transitional environment between the weathered ultramafic substrate and the Fe-rich limonite zone, where secondary immobilization processes begin to dominate.

In Table 3, it can be seen that the enrichment in the saprolite zone is 2.36 times that of the bedrock zone and 2.97 times that of the limonite zone compared to the saprolite zone. Meanwhile, for the total enrichment of the bedrock into limonite, the scandium concentration level increased by an average of around 6.97 times. The enrichment level in each type of bedrock has a value that is not much different, except for Gabbro bedrock which has a much lower enrichment value compared to the enrichment level that occurs in ultramafic bedrock, although the presence of scandium elements present in the Gabbro rock group is the highest compared to other rock groups, due to the presence of high clinopyroxene minerals in this rock as a source of scandium itself, but the level of scandium enrichment in gabbro rock is very low.

Table 3. The level of scandium enrichment in each laterite zone and rock group.

Dunite			**Harzburgite**		
Bedrock	Saprolite	Limonite	Bedrock	Saprolite	Limonite
5.83 ppm	18.95 ppm	44.55 ppm	7.03 ppm	14.29 ppm	47.86 ppm
S/B	L/S	L/B	S/B	L/S	L/B
3.25	**2.35**	**7.64**	**2.03**	**3.35**	**6.81**
Wehrlite			**Lherzolite**		

 doi:10.20944/preprints202512.1452.v1

Bedrock	Saprolite	Limonite	Bedrock	Saprolite	Limonite
5.26 ppm	12.09 ppm	48.28 ppm	5.81ppm	12.27 ppm	46.89 ppm
S/B	L/S	L/B	S/B	L/S	L/B
2.30	**3.99**	**9.18**	**2.11**	**3.82**	**8.07**
Serpentinite			**Gabbro**		
Bedrock	Saprolite	Limonite	Bedrock	Saprolite	Limonite
6.33 ppm	19.28 ppm	48.05 ppm	23.25 ppm	32.5 ppm	58.5 ppm
S/B	L/S	L/B	S/B	L/S	L/B
3.05	**2.49**	**7.59**	**1.40**	**1.80**	**2.52**

(Note: S/B is the ratio between saprolite to bedrock; L/S is is the ratio between limonite to saprolite; L/B is the ratio between limonite to bedrock).

In the comparison chart of the main elements in laterization in the test area (Figure 9), Fe levels are the main factor that carries the scandium element from the bedrock zone to the limonite. however, there are two additional elements that are anomalies that occur in the study area, namely chromium and manganese. in the distribution pattern of elements in the bedrock, saprolite zone, and limonite zone in the study area, it can be seen that in the saprolite zone, the presence of manganese and chromium elements has an average low content in gabbro, wehrlite, and lherzolite rocks, while in dunite and serpentinite there is a fairly high presence of chromium and manganese in the saprolite zone. in the limonite zone, there is a visible anomaly in the presence of chromium and manganese in the gabbro, wehrlite, and lherzolite rock groups.

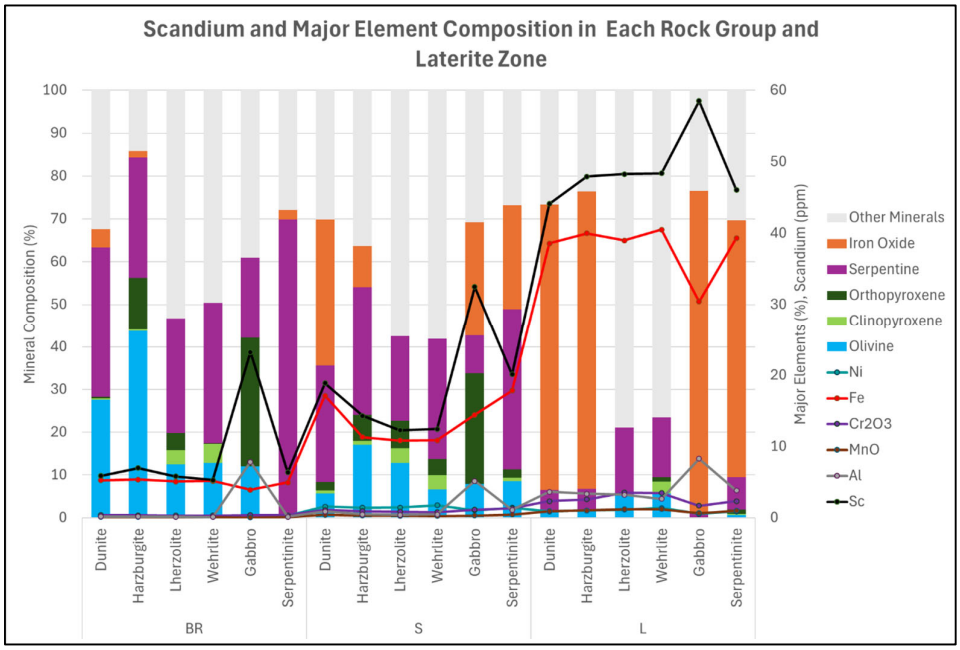

Figure 10. Scandium and major element composition in each rock group and laterite zone.

4.4. Implication for the Exploration in Wailukum Area

[17] reported that clinopyroxene-rich lithologies exhibit a high potential for scandium (Sc) mineralization, as intense chemical weathering can effectively liberate Sc from the protolith and promote its accumulation in the regolith. In the Wailukum area, such clinopyroxene-rich lithologies are primarily represented by gabbro and harzburgite units (Figure 7; Table 1). Considering that scandium grades in known laterite deposits range from approximately 33 ppm in the Shazi deposit, China, to nearly 300 ppm in the Lucknow deposit, Australia [17] and [23,24], the scandium concentrations identified in Wailukum are ranging from 44.55 to 58.50 ppm, this results suggest that this area may hold economically significant potential.

 doi:10.20944/preprints202512.1452.v1

However, further detailed geochemical characterization and systematic exploration are required to delineate the most prospective zones and assess the resource potential accurately. In addition, bulk geochemical data (Figure 8) show a positive correlation between Sc, Ni, and Fe_2O_3, indicating that bulk Ni and Fe_2O_3 contents may serve as useful geochemical proxies for Sc enrichment. Nevertheless, additional investigations are needed to validate these relationships and establish a more robust geochemical indicator framework for scandium mineralization in the region.

5. Conclusions

The findings of this study demonstrate that scandium distribution in the Wailukum area is strongly influenced by host rock type and mineral composition. Gabbro contains the highest absolute scandium concentrations, with 23.25 ppm in the bedrock, 32.5 ppm in the saprolite, and 58.5 ppm in the limonite. This reflects the role of clinopyroxene-rich rocks as primary scandium sources. However, the enrichment ratio in gabbro is relatively low (2.52), suggesting limited mobilization of scandium during lateritization.

In contrast, wehrlite shows the highest relative enrichment, with scandium increasing up to 9.18 times from bedrock to limonite, despite its lower starting content. This indicates that lithologies with less stable primary minerals release scandium more effectively during weathering, allowing for greater accumulation in lateritic horizons. Thus, while gabbro demonstrates the highest absolute values, ultramafic rocks such as wehrlite reveal stronger enrichment potential.

Scandium enrichment is controlled by both primary and secondary minerals. Clinopyroxene serves as the main host in the bedrock, but during lateritization, scandium is transferred and fixed within secondary Fe-, Cr-, and Mn-oxides such as goethite, hematite, magnetite, chromite, and asbolane. These oxides dominate in the limonite zone and act as stable repositories for scandium, making it the key horizon for enrichment regardless of variations in initial bedrock content.

Author Contributions: Conceptualization, A.B., M.F.R., E.T.Y., and A.K.; methodology, A.B.; software, M.C.R.M.; validation, A.B., M.F.R., E.T.Y., and A.K.; formal analysis, A.B, R.A.Y.; investigation, A.B., T.R.U.; writing—original draft preparation, A.B.; writing—review and editing, A.B, M.F.R., E.T.Y., and A.K.; visualization, A.B., R.A.Y., M.C.R.M., and T.R.U.; supervision, M.F.R., E.T.Y., and A.K; project administration, A.B.; funding acquisition, A.B. All authors have read and agreed to the published version of the manuscript.

Funding: This research was funded by PT Antam Tbk.

Data Availability Statement: All relevant data are in this paper.

Acknowledgments: We would like to express our sincere gratitude to PT. ANTAM for their permission and support to this research in the Pongkor gold mine. Special thanks are given to Andi Kurniawan, Syaiful Hilal, Duduk Sumargono, Reza Rizqie Ramadhan, and Naafiakra Nouval their invaluable support during the fieldwork and desktop study. We also very grateful for the generous support from PT Antam Tbk for their funding in this research analysis.

Conflicts of Interest: The research was conducted on the Wailukum area, owned by PT Aneka Tambang Tbk, with which Abdul Bari, Rubima Aisha Yulman, Muhammad Chandra RM, and Thaha Riza Ulhaq are affiliated. Although this affiliation may present a potential conflict of interest, the authors affirm that the research was conducted transparently, with adherence to ethical guidelines, and that every effort was made to maintain objectivity and minimize bias in the study design, data collection, analysis, and interpretation. The remaining authors declare no conflicts of interest.

 doi:10.20944/preprints202512.1452.v1

Appendix A

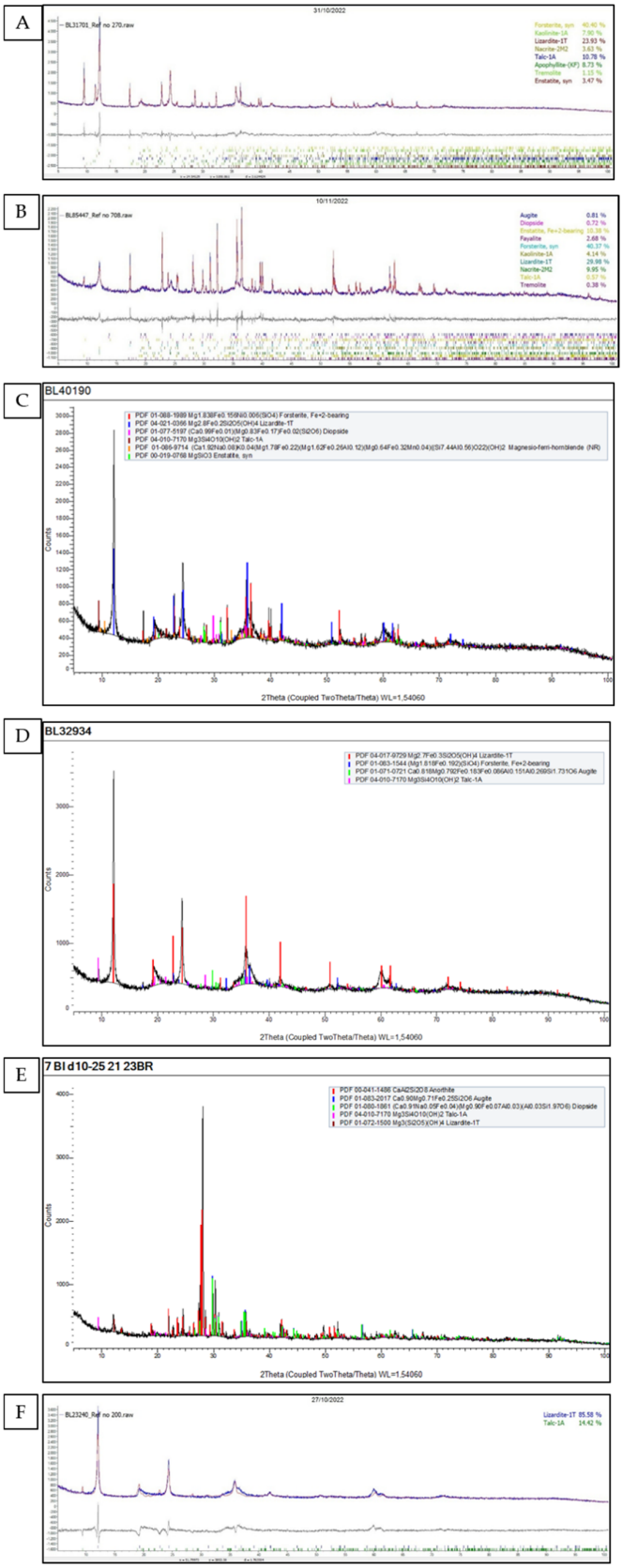

Figure A1. (A-F) Rietveld refinement for all type (type 1 – 6) XRD spectrum in Wailukum.

 doi:10.20944/preprints202512.1452.v1

References

1. Ito, A., Otake, T., Maulana A., Sanematsu K., Sufriadin, Sato, T. (2021). Geochemical constraints on the mobilization of Ni andcritical metals in laterite deposits, Sulawesi, Indonesia:A mass-balance approach. Resource Geology Volume 71, Issue 3, 177-282.
2. Maulana, A., Sanematsu, K., & Sakakibara, M. (2019). Study on Sc-bearing Lateritic Ni deposits in Ultramafic Rock from Sulawesi: A New Paradigm in Indonesia Metal Mining Industry. IOP Conference Series: Materials Science and Engineering, 676(1), 012032.
3. Riggall, S. (2015). Australian scandium supply—A paradigm shift for a strategic metal. In Proceedings of the Latest Word on Aerospace Materials, Long Beach, CA, USA, 11–14 May 2015.
4. Onggang, S., Maulana, A., & Irfan, U. R. (2021). Preliminary Study of Scandium Enrichment in Lateritic Profile from Weathered Ultramafic Rock in Lapaopao Area Kolaka Regency of Southeast Sulawesi. IOP Conference Series: Earth and Environmental Science, 921(1), 012040.
5. Teitler, Y., Cathelineau, M., Ulrich, M., Ambrosi, J. P., Munoz, M., & Sevin, B. (2019). Petrology and geochemistry of scandium in New Caledonian Ni-Co laterites. Journal of Geochemical Exploration, 196, 131–155.
6. Chassé, M., Griffin, W. L., O'Reilly, S. Y., & Calas, G. (2016). Scandium speciation in a world-class lateritic deposit. Geochemical Perspectives Letters, 3(2), 105–114.
7. Maulana, A., Sanematsu, K., & Sakakibara, M. (2016). An overview on the possibility of scandium and REE occurrence in Sulawesi, Indonesia. Indonesian Journal on Geoscience, 3(2), 139–147.
8. Stueber, A. M., & Goles, G. G. (1967). Abundances of Na, Mn, Cr, Sc and Co in ultramafic rocks. Geochimica et Cosmochimica Acta, 31(1), 75–93.
9. Hall, R. (2000). Neogene History of Collision in The Halmahera Region, Indonesia. Proceedings of the Indonesian Petroleum Association 27th Annual Convention, 487-493.
10. Darman, H. (2000). An outline of the geology of Indonesia. Lereng Nusantara. https://books.google.com/books?hl=en&lr=&id=NyqDDwAAQBAJ&oi=fnd&pg=PP2&dq=Sukamto+et+al.,+1981+dalam+Darman+%26+Sidi,+2000&ots=UgvtDwCwqG&sig=M7u40Y5bu4x-wBCDlYz8jeBygww
11. Antam. (2022). Exploration progress report in Pongkor Au-Ag mine, West Java, Indonesia. Internal report (unpublished manuscript).
12. Apandi, T. & Sudana, D. 1980. Geologic map of the Ternate quadrangle, North Maluku. Geological Research and Development Centre, Bandung, Indonesia.
13. Streckeisen, A. (1975). How should charnockitic rocks be named? Annales de La Société Géologique de Belgique. https://popups.uliege.be/0037-9395/index.php?id=3742
14. Sufriadin, Widodo, S., Jaya, A., & Azman. (2022, November). The effect of heating on mineral and chemical composition of saprolite ore from Latowu area, North Kolaka regency of Southeast Sulawesi, Indonesia. In *AIP Conference Proceedings* (Vol. 2543, No. 1, p. 050006). AIP Publishing LLC.
15. Marsh, E. E., Anderson, E. D., & Gray, F. (2011). *Ni-Co Laterites: A Deposit Model*. Denver, CO: US Department of the Interior, US Geological Survey.
16. El Mendili, Y., Chateigner, D., Orberger, B., Gascoin, S., Bardeau, J. F., Petit, S., ... & Pilliere, H. (2019). Combined XRF, XRD, SEM-EDS, and Raman analyses on serpentinized harzburgite (nickel laterite mine, New Caledonia): Implications for exploration and geometallurgy. *ACS Earth and Space Chemistry*, *3*(10), 2237-2249.
17. Wang, Z., Li, M. Y. H., Liu, Z. R. R., & Zhou, M. F. (2021). Scandium: Ore deposits, the pivotal role of magmatic enrichment and future exploration. *Ore Geology Reviews*, *128*, 103906.
18. Chassé, M., Griffin, W. L., O'Reilly, S. Y., & Calas, G. (2019). Australian laterites reveal mechanisms governing scandium dynamics in the critical zone. *Geochimica et Cosmochimica Acta*, *260*, 292-310
19. Qin, H. B., Yang, S., Tanaka, M., Sanematsu, K., Arcilla, C., & Takahashi, Y. (2021). Scandium immobilization by goethite: Surface adsorption versus structural incorporation. *Geochimica et Cosmochimica Acta*, *294*, 255-272.
20. Teitler, Y., Cathelineau, M., Ulrich, M., Ambrosi, J. P., Munoz, M., & Sevin, B. (2019). Petrology and geochemistry of scandium in New Caledonian Ni-Co laterites. *Journal of Geochemical Exploration*, *196*, 131-155.

 doi:10.20944/preprints202512.1452.v1

21. Goldich, S. S. (1938). A study in rock-weathering. *The Journal of Geology*, *46*(1), 17-58.
22. Shepherd, K., Namur, O., Toplis, M. J., Devidal, J. L., & Charlier, B. (2022). Trace element partitioning between clinopyroxene, magnetite, ilmenite and ferrobasaltic to dacitic magmas: an experimental study on the role of oxygen fugacity and melt composition. *Contributions to Mineralogy and Petrology*, *177*(9), 90.
23. Hoatson, D. M., Jaireth, S., & Miezitis, Y. (2011). The major rare-earth-element deposits of Australia: geological setting, exploration, and resources. Geoscience Australia.
24. Nie, A. G., Sun, J., & Zhang, M. (2018). Analysis of forming conditions and genesis of Sazi independent scandium deposit in Qinglong, Guizhou Province. *Journal of Guizhou University (Natural Sciences)*, *35*(5), 31-36.